WP12

Theoretical Methods for Condensed Matter

Part III

Tom Frömbgen

Assistants: Katharina Bauerfeind & Berenike Stahl

Submission 1: January 7, 2022

1 Bulk Properties of NaCl

As part of this practical computational course, bulk properties of sodium chloride such as lattice parameters, atomization energies, band gaps and densities of states were computed. All calculations were performed using the CRYSTAL program package.[1,2] An experimental crystal structure of sodium chloride was taken from the Crystallography Open Database[3] (COD-ID: 9006369). This specific structure was chosen as experimental input because it was measured at 298 K which was closest to the optimum temperature of 0 K (temperature of the calculations).

1.1 Structural relaxation

Full structural relaxations on the LDA/VWN,[4] PWGGA,[5] M06L[6] and PBE0[7] level of theory employing POB-DZVP-rev2 basis sets[8] were performed. Results are summarized in Table 1. The LDA/VWN functional strongly underestimates the reference value of $a_{\text{exp}} = 5.5937$ Å which can be deduced to the overbinding nature of the functional. Improvement comes with the meta-GGA functional M06L which nevertheless underestimates the lattice parameter by more than 1 %. Good accuracy is reached by PWGGA and PBE0. The latter hybrid functional comes with a largely increased computation time which is about four times larger compared to the other functionals. In conclusion, it can be said that reasonable geometries do not require the use of hybrid functionals but can also be obtained from certain (meta-)GGA functionals. This is also well known for geometry optimization of molecules.[9,10]

Table 1: Full structural relaxations of NaCl: Functional, computational time (min), lattice parameter a (Å), deviation from experimental value Δa (%)

Functional	comp time	a	Δa
LDA/VWN	3.04	5.410	-3.28
M06L	3.12	5.492	-1.82
PBE0	16.2	5.573	-0.37
PWGGA	3.26	5.614	0.37

1.2 Atomization energy

The atomization energy of sodium chloride was computed employing PBE0 and POB-TZVP-rev2 basis sets.[8] To do so, the atomic basis sets were enlarged by adding *s, p* and *d* shells until the atomic energies $E_{\text{Na}}, E_{\text{Cl}}$ were converged to a limit of 1 kcal/mol. Having reached the desired convergence, an atomization energy $\Delta E^{\text{atom}}_{\text{NaCl}}$ of 623.3 kJ/mol was obtained according to

$$\Delta E^{\text{atom}}_{\text{NaCl}} = E_{\text{NaCl}} - E_{\text{Na}} - E_{\text{Cl}} \tag{1}$$

as displayed in Table 2. This value represents an electronic energy and cannot be directly compared to an experimental quantity which is usually the atomization enthalpy $\Delta \text{H}^0_{\text{atom}}(\text{NaCl})$.

Table 2: Energies of a sodium E_{Na} and chlorine E_{Cl} atom, sodium chloride E_{NaCl} (all in E_{h}) and the atomization energy of sodium chloride $\Delta E^{\mathrm{atom}}_{\mathrm{NaCl}}$ (kJ/mol).

E_{Na}	E_{Na}	E_{NaCl}	$\Delta E^{\mathrm{atom}}_{\mathrm{NaCl}}$
-162.17	-459.98	-622.39	623.34

Comparison is achieved according to the Born–Haber circle by adding the sublimation enthalpy of sodium $\Delta \mathrm{H}^0_{\mathrm{subl}}(\mathrm{Na}) = 107.3\,\mathrm{kJ/mol}$ and half of the dissociation enthalpy of chlorine $\Delta \mathrm{H}^0_{\mathrm{diss}}(\mathrm{Cl_2}) = 121.3\,\mathrm{kJ/mol}$ to the negative enthalpy of formation of sodium chloride $\Delta_{\mathrm{f}}\mathrm{H}^0_{\mathrm{solid}}(\mathrm{NaCl}) = -411.1\,\mathrm{kJ/mol}$ (all values taken from the NIST chemistry webbook[11]):

$$\Delta \mathrm{H}^0_{\mathrm{atom}}(\mathrm{NaCl}) = -\Delta_{\mathrm{f}}\mathrm{H}^0_{\mathrm{solid}}(\mathrm{NaCl}) + \frac{1}{2}\Delta \mathrm{H}^0_{\mathrm{diss}}(\mathrm{Cl_2}) + \Delta \mathrm{H}^0_{\mathrm{subl}}(\mathrm{Na}) \tag{2}$$

This results in $\Delta \mathrm{H}^0_{\mathrm{atom}}(\mathrm{NaCl}) = 639.7\,\mathrm{kJ\,mol^{-1}}$. The atomization energy differs from that by $-2.5\,\%$ which is deduced to the fact that atomization energy and enthalpy are per definition not identical. Thermal corrections need to be added to make the values comparable.

1.3 Band gap

Band gaps of sodium chloride were computed on a PW1PW[12]/POB-TZVP,[13] PBE0/POB-TZVP, and PBE0/mTZVP[14] level of theory. The band gaps were first calculated with the standard amount of Fock exchange α included in the respective functionals. Subsequently, self-consistent hybrid calculations were performed in order to determine the optimal amount of Fock exchange. Having obtained this information, band gaps were computed using the optimal amount of Fock exchange. Results are summarized in Table 3. Note that the inverse of α corresponds to the dielectric constant ε.

Table 3: Calculated band gaps of sodium chloride (eV), amount of Fock exchange α and dielectric constant ε.

Method	Band gap	α	ε
PBE0/mTZVP	7.28	0.25	4.00
PBE0/mTZVP	8.89	0.49	2.05
PBE0/POB-TZVP	7.66	0.25	4.00
PBE0/POB-TZVP	9.51	0.46	2.18
PW1PW/POB-TZVP	7.23	0.20	5.00
PW1PW/POB-TZVP	9.50	0.46	2.19

During the past six decades, numerous experimental band gaps have been reported in the literature[15] mostly ranging from 8.4 to 9.0 eV. It can be seen that the quality of the calculated

band gaps significantly increases upon using the optimized amount of Fock exchange. While all tested method with standard amount of Fock exchange underestimate the experimental band gaps, PBE0/mTZVP with an optimal amount of Fock exchange is well in the range of the reported reference values. However, PBE0/POB-TZVP and PW1PW/POB-TZVP with an optimal amount of Fock exchange overestimate the band gap but not as much as it was underestimated before. Hence, an mTZVP seems to be more suitable for this kind of calculation. A reason might be found in the missing diffuse functions in POB-TZVP in order to avoid linear dependencies in solid state calculations. Despite the increased accuracy, one has to keep the rather large computational effort of self-consistent hybrid calculations in mind.

1.4 Projected density of states

The projected density of states (PDOS) of sodium chloride was computed on a PBE0/POB-TZVP level of theory with standard and optimal amount of Fock exchange (as given in Table 3). It is displayed in Figure 1.

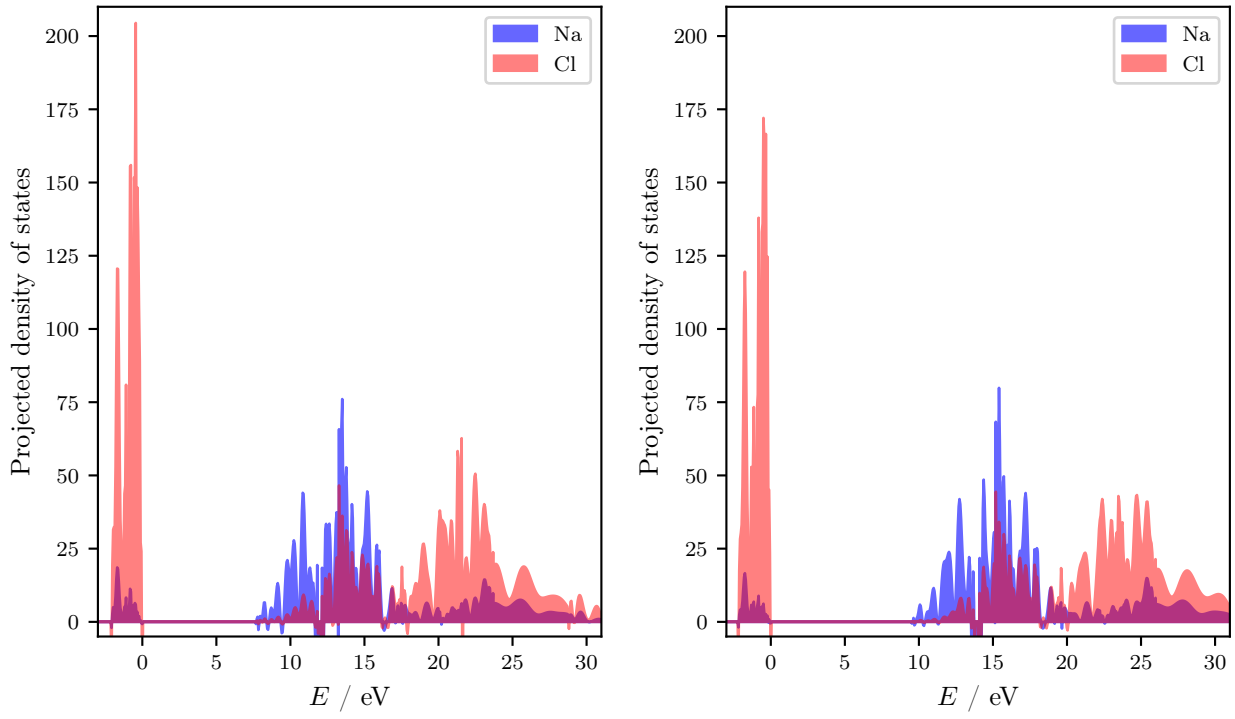

Figure 1: Projected density of states of NaCl on a PBE0/POB-TZVP level of theory with standard (left) and optimal Fock exchange fraction (right) obtained by a self-consistent hybrid calculation (see Table 3).

Generally, both PDOS plots look quite similar. The unoccupied crystal orbitals in the conduction band of the PDOS with optimal amount of Fock exchange are shifted to the right by 1.9 eV as compared to the other one due to the larger band gap. In both cases, the valence band is dominated by chlorine and whereas sodium dominates the lower energy part of the conduction

band. By that, in can be concluded that the highest occupied crystal orbital (HOCO) is mainly chlorine-centered and the lowest unoccupied crystal orbital (LUCO) is mainly sodium-centered. This observation is in line with the common understanding of the ionic sodium chloride crystal: Sodium donates its atoms to chlorine and is therefore present as Na^+, whereas chlorine forms Cl^-. Due to the electron deficient nature of the Na^+ it is straight forward that its orbitals are higher in energy than those of the electron rich Cl^- anion.

2 Calculating surfaces of Rutile

The second part of this course dealt with the investigation of low-index rutile TiO_2 surfaces including structural relaxations, slab models and surface energies as well as a Wulff construction. All calculations were performed using the CRYSTAL program package. The Wulff construction was done with VESTA.[16] An experimental crystal structure of rutile was taken from the Crystallography Open Database (COD-ID: 9004141). This specific structure was chosen as experimental input because it was measured at 25 K which was closest to the optimum temperature of 0 K (temperature of the calculations).

2.1 Structural relaxation

Full structural relaxations on the PBE0, PWGGA, PBESOL[17] and PW1PW level of theory employing POB-TZVP-rev2 (rev2) and the CRYSTAL standard (std) basis sets were performed. Results are summarized in Table 4.

Table 4: Full relaxations of rutile: Method, computation time (min), lattice parameter a, c (Å) and their deviation from experiment $\Delta a, \Delta c$ (%) as well as the fractional x coordinate of oxygen.

Method	comp time	a	Δa	c	Δc	x_{frac}(O)
PBE0/rev2	344.76	4.578	-0.33	2.951	-0.28	0.305
PBESOL/rev2	19.01	4.589	-0.08	2.946	-0.42	0.304
PW1PW/rev2	328.13	4.585	-0.18	2.953	-0.2	0.305
PWGGA/rev2	57.42	4.634	0.89	2.969	0.34	0.305
PBE0/std	184.25	4.565	-0.62	2.981	0.74	0.304
PBESOL/std	13.97	4.577	-0.35	2.970	0.39	0.304
PW1PW/std	219.18	4.571	-0.47	2.982	0.77	0.304
PWGGA/std	23.77	4.617	0.51	2.993	1.16	0.304

All tested methods give reasonable results for the lattice parameters a, c since they are - except for PWGGA/std at c - within 1 % accuracy compared to the reference data of $a_{\text{exp}} = 4.593$ Å and $c_{\text{exp}} = 2.959$ Å. There are some general trends observable: rev2 results are more accurate than std results which justifies the usage of the former basis sets instead of the CRYSTAL default basis sets. The PWGGA functional is too repulsive and results in too large lattice parameters for both basis sets. The other GGA functional PBESOL yields better results and slightly underestimates the lattice parameters, except for c with the worse std basis sets. In contrast to that, the two investigated hybrid functionals do not perform systematically better than their GGA competitors. Instead, they perform even worse than PBESOL in most cases. Taking a look at the computed fractional x coordinates of the oxygen atoms, all investigated methods

obtain identical results. The differences are very small and negligible. The observation that hybrid functionals do not happen to be necessarily better than GGA functionals with regard to geometry optimizations was also found for NaCl and discussed before - especially, when noting the largely increased computation times.

2.2 Surface energy

Having received the information that PBESOL/rev2 is an accurate and cheap level of theory for geometry optimizations of rutile, low-index surfaces of rutile were investigated with this method. Surfaces were generated with the *SLABCUT* option and specified by the parameters L, S which denote the starting layer and the number of atomic layers that form the surface, respectively. The surface slabs need to fulfill requirements in order to make the computation feasible. They

- must be symmetric and conserve the symmetry of the underlying crystal structure (rutile)
- must be stoichiometric w.r.t the sum formula of the compound (TiO_2)
- must not possess a dipole moment in z direction (the surfaces are formally formed in the xy plane)

Obeying these criteria, only certain values for L, S are possible. These are depicted in Table 5.

Table 5: Allowed values for L, S in the definition of slab models of low-index rutile surfaces ($j \in \mathbb{N}$).

Surface	L	S
001	1	j
100	2	$3j$
101	2	$3j$
110	2	$3j$

After having computed slab models consisting out of two to eight stoichiometric layers for the four given surfaces, the surface energy E_{surf} can be obtained as

$$E_{\text{surf}}(n) = \frac{E_{\text{slab}}(n) - n \cdot E_{\text{bulk}}}{2A} \tag{3}$$

where n denotes the number of stoichiometric layers, E_{slab} is the slab energy, E_{bulk} the bulk energy (3D system) and A is the area of the employed surface model. The surface energy oscillates and converges to the exact value with an increasing (and sufficiently large) number of stoichiometric layers. For reasons of convenience, the surface energies are not given in tables but in Figure 2. The computed surface energies are in good agreement with the literature.[18]

They were supposed to be specifically compared to PW1PW/rev2 results (but for the largest surface model only). This is given in Table 6. In case of the (001) and (101) surface, both methods agree on the surface energy. They do deviate in case of (100) and (110). Taking a look the above-mentioned literature, it can be seen that converging the surface energy requires more than eight stoichiometric layers. Therefore, the obtained results are considered acceptable.

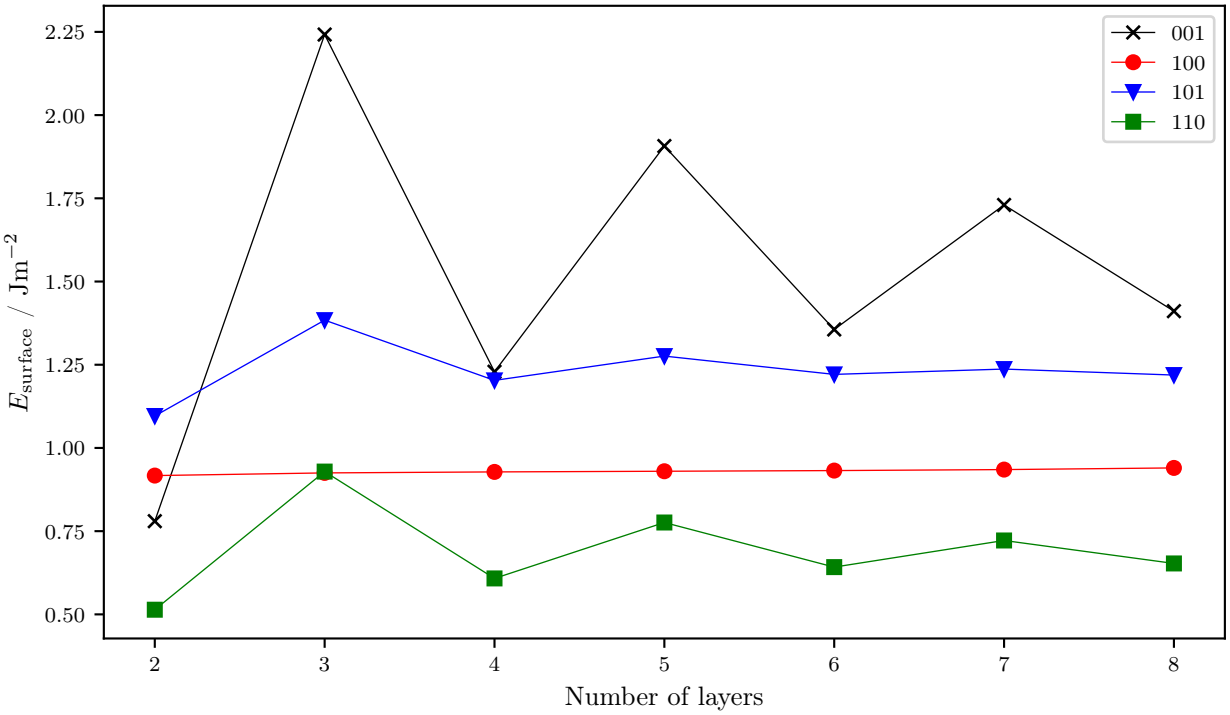

Figure 2: Calculated surface energies for different TiO_2 surfaces.

Table 6: Surface energies of rutile: Surface, number of layers n, energies computed with PBESOL and PW1PW $E_{\text{PBESOL}}, E_{\text{PW1PW}}$ (in J/m^2).

Surface	n	E_{PBESOL}	E_{PW1PW}
001	8	1.411	1.407
100	8	0.935	0.845
101	8	1.237	1.190
110	8	0.722	0.592

Furthermore, the relaxation of symmetry-nonequivalent atoms in z direction was to be investigated for the (110) surface, where relaxation denotes the difference between the relaxed (optimized) and the initial (non-relaxed) structure. The relaxations are displayed in Figure 3. Taking a look at the three distinct atoms in the topmost layer of the surface models first, it is observed that the Ti3 atoms move to larger distances whereas the Ti2 atoms show a negative Δz. The oxygen atoms mostly show a slightly positive relaxation. Again, oscillations of

the values are observed. This means that the TiO_6 octahedra are remarkably distorted at the borders of the surface models.

For Ti2 and Ti3, a similar behavior is observed for the bulk-like atoms in the middle of the surface models: These atoms show large oscillating relaxations counteracting each other. Opposed to that, the oxygen atoms nearly do not relax except for O4/5 at $n = 3$ but stay close to their original positions. This leads to distortions of the TiO_6 octahedra which are different to those at the topmost layers. The computed relaxations are in good agreement with the literature.[18]

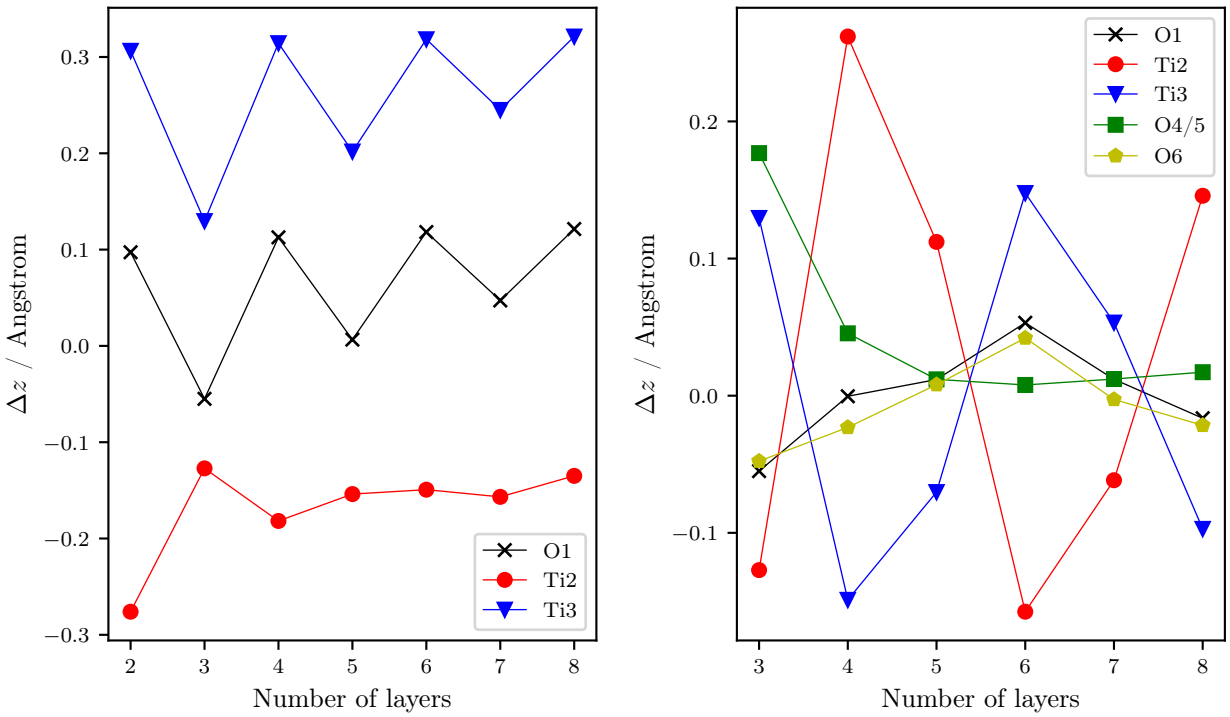

Figure 3: Relaxation of symmetry-nonequivalent atoms in TiO_2 (110) surfaces of different thickness: Atoms in the topmost layer (left) are compared to bulk-like atoms in middle layers (right).

2.3 Crystal shape

Finally, the calculated surface energies are used to generate a graphical representation of the rutile crystal shape. According to Wulff's theorem, the length of a vector normal to a crystal face is proportional to its surface energy. Hence, knowing the surface energy of a sufficient number of surfaces enables a reliable representation of the crystal shape. The result is displayed in Figure 4 and compared to experimental data which are in nice agreement. Therefore, the presented approach to access surface energies and thereby the crystal shape are considered reasonable.

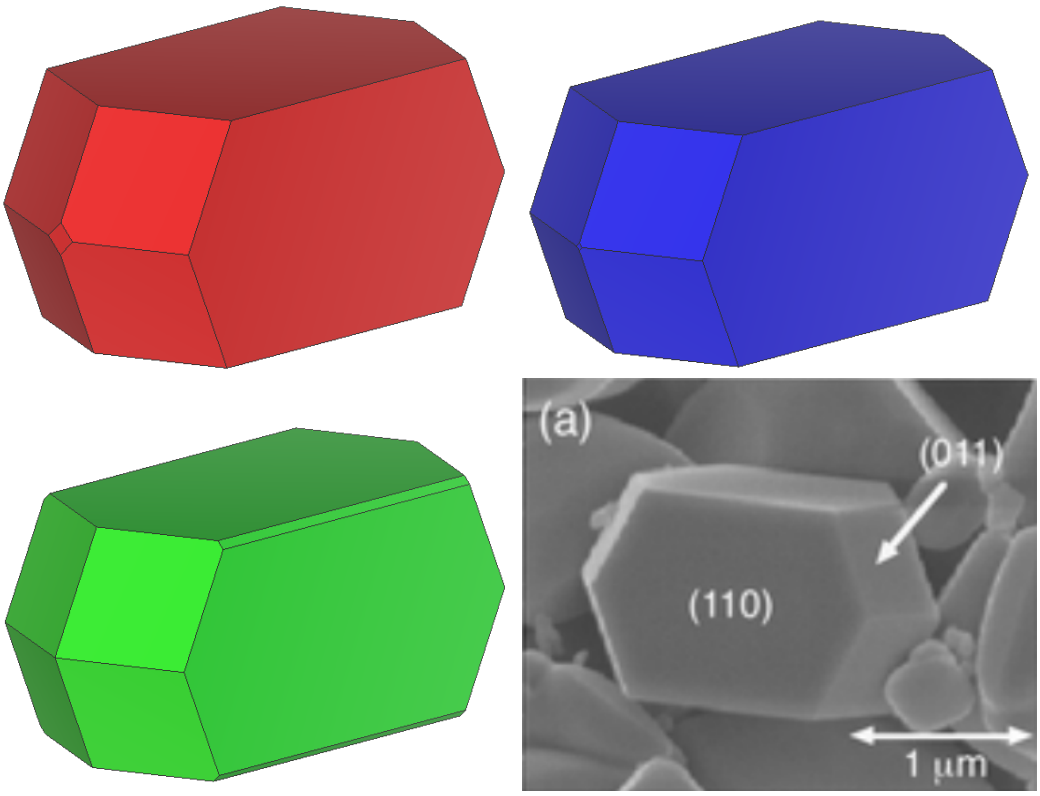

Figure 4: Crystal shape of rutile: Wulff construction based on the surface energies calculated with PBESOL (top left), PW1PW (top right), theoretical literature[18] (bottom left) and comparison to experimental data[19] (bottom right).

Literature

[1] R. Dovesi, A. Erba, R. Orlando, C. M. Zicovich-Wilson, B. Civalleri, L. Maschio, M. Rérat, S. Casassa, J. Baima, S. Salustro, et al., *Wiley Interdiscip. Rev. Comput. Mol. Sci.* **2018**, *8*, e1360.

[2] R. Dovesi, V. Saunders, C. Roetti, R. Orlando, C. Zicovich-Wilson, F. Pascale, B. Civalleri, K. Doll, N. Harrison, I. Bush, et al., **2017**.

[3] Crystallography Open Database, `http://www.crystallography.net/cod/`.

[4] S. H. Vosko, L. Wilk, M. Nusair, *Can. J. Phys.* **1980**, *58*, 1200–1211.

[5] J. P. Perdew, J. A. Chevary, S. H. Vosko, K. A. Jackson, M. R. Pederson, D. J. Singh, C. Fiolhais, *Phys. Rev. B* **1992**, *46*, 6671.

[6] Y. Zhao, D. G. Truhlar, *J. Chem. Phys.* **2006**, *125*, 194101.

[7] C. Adamo, V. Barone, *J. Chem. Phys.* **1999**, *110*, 6158–6170.

[8] D. Vilela Oliveira, J. Laun, M. F. Peintinger, T. Bredow, *J. Comp. Chem.* **2019**, *40*, 2364–2376.

[9] J. Tao, J. P. Perdew, V. N. Staroverov, G. E. Scuseria, *Phys. Rev. Lett.* **2003**, *91*, 146401.

[10] S. Grimme, A. Hansen, S. Ehlert, J.-M. Mewes, *J. Chem. Phys.* **2021**, *154*, 064103.

[11] NIST Chemistry WebBook, `https://webbook.nist.gov/chemistry/`.

[12] T. Bredow, A. R. Gerson, *Phys. Rev. B* **2000**, *61*, 5194.

[13] M. F. Peintinger, D. V. Oliveira, T. Bredow, *J. Comp. Chem.* **2013**, *34*, 451–459.

[14] J. G. Brandenburg, C. Bannwarth, A. Hansen, S. Grimme, *J. Chem. Phys.* **2018**, *148*, 064104.

[15] M. Hochheim, T. Bredow, *Phys. Rev. B* **2018**, *97*, 235447.

[16] K. Momma, F. Izumi, *J. Appl. Crystallogr.* **2011**, *44*, 1272–1276.

[17] J. P. Perdew, A. Ruzsinszky, G. I. Csonka, O. A. Vydrov, G. E. Scuseria, L. A. Constantin, X. Zhou, K. Burke, *Phys. Rev. Lett.* **2008**, *100*, 136406.

[18] T. R. Esch, I. Gadaczek, T. Bredow, *Appl. Surf. Sci.* **2014**, *288*, 275–287.

[19] T. Ohno, K. Sarukawa, M. Matsumura, *New J. Chem.* **2002**, *26*, 1167–1170.